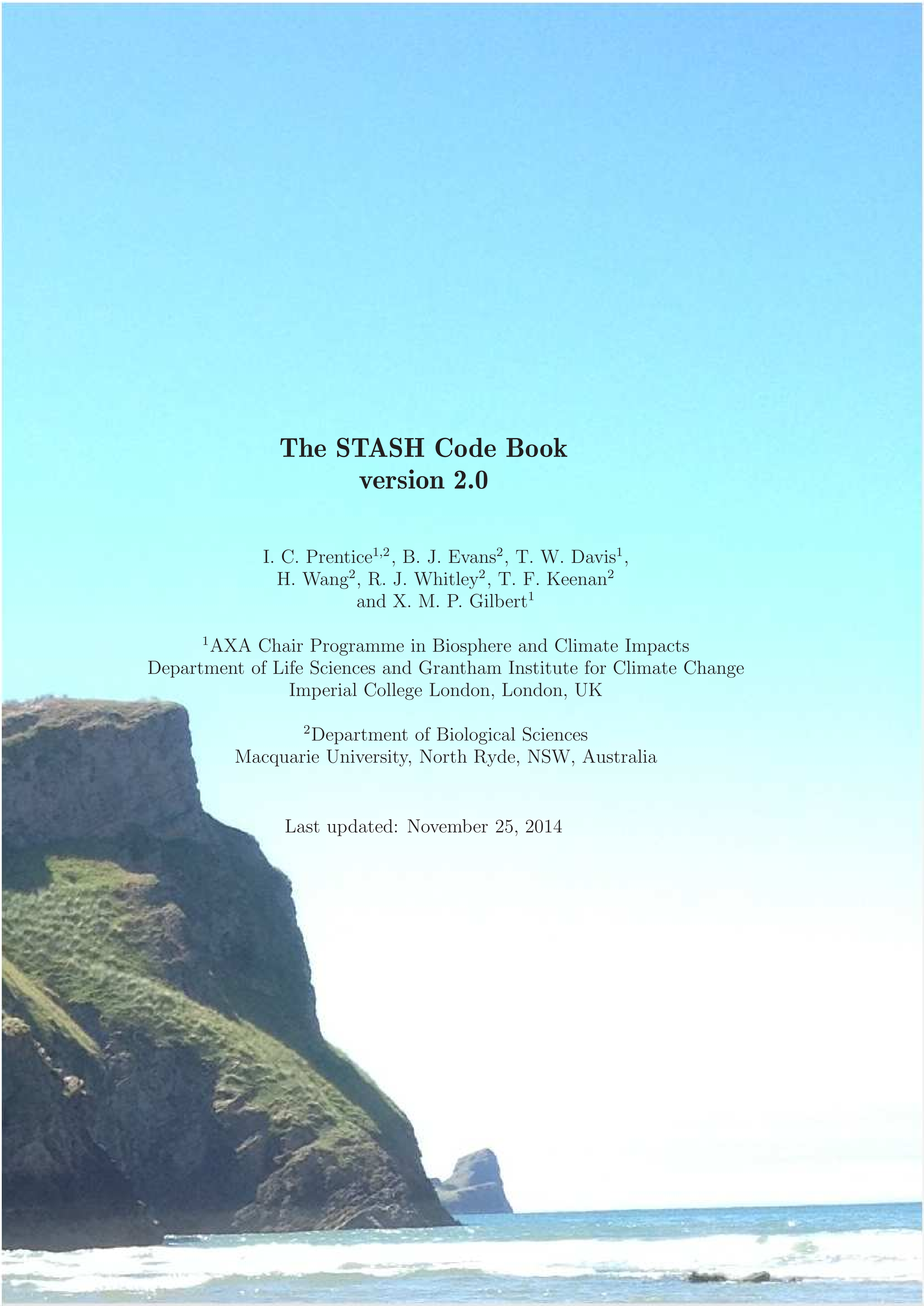

The STASH Code Book
version 2.0

I. C. Prentice[1,2], B. J. Evans[2], T. W. Davis[1],
H. Wang[2], R. J. Whitley[2], T. F. Keenan[2]
and X. M. P. Gilbert[1]

[1]AXA Chair Programme in Biosphere and Climate Impacts
Department of Life Sciences and Grantham Institute for Climate Change
Imperial College London, London, UK

[2]Department of Biological Sciences
Macquarie University, North Ryde, NSW, Australia

Last updated: November 25, 2014

Contents

List of Notations

1 Introduction

This work aims to model monthly global radiation, evaporation, and soil moisture quantities and indexes using simple but theoretically-based simulation.

1.1 Theory

The methodology is based on the psuedo-code presented by (Cramer and Prentice 1988):

1. Daily
   (a) Estimate the evaporative supply rate, S_w (§2.2)
   (b) Calculate (or estimate) the heliocentric longitudes, ν and λ (§2.3.6)
   (c) Calculate (or estimate) the distance factor, d_r (§2.3.2)
   (d) Calculate (or estimate) the declination angle, δ (§2.3.4)
   (e) Calculate the sunset angle, h_s (Eq. 41)
   (f) Calculate daily extraterrestrial solar radiation flux, H_o (§2.4)
   (g) Estimate transmittivity, τ (§2.5.1)
   (h) Calculate daily photosynthetic photon flux density, Q_n (§2.8)
   (i) Estimate net longwave radiation flux, I_{LW} (§2.5)
   (j) Calculate net radiation cross-over hour angle, h_n (Eq. 54)
   (k) Calculate daytime net radiation, H_N (§2.6)
   (l) Calculate nighttime net radiation, H_N^* (§2.7)
   (m) Calculate energy conversion factor, E_{con} (§2.9)
   (n) Estimate daily condensation, C_n (§2.10)
   (o) Estimate daily equilibrium evapotranspiration, E_n^q (§2.12)
   (p) Estimate daily potential evapotranspiration, E_n^p (§2.14)
   (q) Calculate the intersection hour angle, h_i (Eq. 83)
   (r) Estimate daily actual evapotranspiration, E_n^a (§2.17)
   (s) Update daily soil moisture, W_n (§2.18)
2. Monthly
   (a) Sum monthly totals of E_m^a, E_m^p, E_m^q and Q_m
   (b) Calculate monthly Cramer-Prentice moisture index, α (§2.19)
   (c) Calculate monthly climatic water deficit, ΔE_m (§2.20)
3. Yearly
   (a) Test whether soil on 31 December agrees with initial conditions

1.2 Key Outputs

The key outputs from this model are:

1. monthly PPFD (Q_m), mol·m^{-2}
2. monthly equilibrium evapotranspiration (E_m^q), mm
3. monthly potential evapotranspiration (E_m^p), mm
4. monthly Cramer-Prentice moisture index (α), unitless
5. monthly climatic water deficit (ΔE_m), mm

1.3 Model Inputs

The model simulation of radiation fluxes requires basic inputs on the time of the year (i.e., year, month, and day) and geographic position (i.e., longitude, θ_{lon}, latitude, ϕ, and elevation, z). For modeling evaporation, the basic meteorological variables needed are: air temperature, precipitation, and fraction of sunlight hours.

In most cases, daily values of the necessary meteorological variables are not available (especially for global coverage). It is possible, then, to use CRU TS datasets[1], which provide 0.5° resolution global monthly climate variables including: monthly mean daily air temperature, °C (TMP), monthly precipitation totals, millimeters (PRE), and percent cloudiness, unitless (CLD).

Based on CRU TS climatic data, the mean daily temperature, T_c, may be assumed constant for each day in the month. The daily precipitation, P_n, may be assumed as a constant fraction of the monthly precipitation (i.e., the monthly total precipitation divided by the number of days in the month, N_m). The percent cloudiness data is derived on fractional sunshine hours (Harris et al. 2014); therefore, the fraction of sunshine hours, S_f, may be calculated (albeit only loosely analogous) as the complementary fraction of cloudiness (i.e., $1-$CLD) and may be assumed constant for each day in the month.

1.4 Model Constants

Table 1 presents the constant values used in this model with the corresponding symbol used in this document and variable name used in the coded environment.

[1] `http://badc.nerc.ac.uk/view/badc.nerc.ac.uk__ATOM__dataent_1256223773328276`

Table 1: Constants used in the STASH model.

Symbol	Variable	Value	Definition
A	`kA`	107	Constant for R_{nl}, W·m^{-2} (Monteith and Unsworth 1990)
a	`ka`	1.49598	Semi-major axis, $\times 10^8$ km (Allen 1973)
β_{sw}	`kalb_sw`	0.17	Shortwave albedo, unitless (Federer 1968)
β_{vis}	`kalb_vis`	0.03	PAR albedo, unitless (Sellers 1985)
b	`kb`	0.20	Constant for R_{nl}, unitless (Linacre 1968)
c	`kc`	0.25	Cloudy transmittivity, unitless (ibid.)
d	`kd`	0.50	Angular coefficient of transmittivity, unitless (ibid.)
e	`ke`	0.01670	Eccentricity (2000 CE), unitless (Berger 1978)
ϵ	`keps`	23.44	Obliquity (2000 CE), degrees (ibid.)
fFEC	`kfFEC`	2.04	From flux to energy, μmol·J^{-1} (Meek et al. 1984)
g	`kG`	9.80665	Gravitational acceleration, m·s^{-2} (Allen 1973)
GM	`kGM`	1.32712	Standard gravity, $\times 10^{11}$ km^3·s^{-2}
I_{sc}	`kGsc`	1360.8	Solar constant, W·m^{-2} (Kopp and Lean 2011)
L	`kL`	0.0065	Lapse rate, K·m^{-1} (Cavcar 2000)
M_a	`kMa`	0.028963	Molecular weight of dry air, kg·mol^{-1} (Tsilingiris 2008)
M_v	`kMv`	0.01802	Molecular weight of water vapor, kg·mol^{-1} (ibid.)
ω	`kw`	0.26	Entrainment, unitless (Lhomme 1997; Priestley and Taylor 1972)
$\tilde{\omega}$	`komega`	283	Longitude of perihelion (2000 CE), degrees (Berger 1978)
P_o	`kPo`	101325	Base pressure, Pa (Cavcar 2000)
R	`kR`	8.3143	Universal gas constant, J·mol^{-1}·K^{-1} (Allen 1973)
σ_{sb}	`ksb`	5.670373	Stefan-Boltzmann constant, $\times 10^{-8}$ W·m^{-2}·K^{-4}
S_c	`kCw`	1.05	Supply constant, mm·hr^{-1} (Federer 1982)
T_o	`kTo`	298.15	Base temperature, K (Prentice, unpublished)

Table 1: Constants used in the STASH model (continued).

Symbol	Variable	Value	Definition
W_m	`kWm`	150	Soil moisture capacity, mm (Cramer and Prentice 1988)

2 Methodology

The following describe the methods of calculating the quantities presented in the theory (§1.1).

2.1 The Julian Day

The Julian day (or Julian date) is a method of continuous numbering of the calendar days based on a certain epoch (e.g., 12-noon on 1 Jan 4713 BC). There are many methods in computer programming languages that allow for the conversion of dates (i.e., year, month, and day) to days. However, if there is none available, the algorithm given in Appendix A.1 (Meeus 1991) will allow for the conversion of calendar dates to Julian days, which will be useful in calculating the number of days in a year, the number of days in a month, and the current day of the year.

To get the number of days in a specific year, N, using the `julian_day` function:

$$N = \text{julian\_day}(y + 1, 1, 1) - \text{julian\_day}(y, 1, 1) \tag{1}$$

where:
N = number of days in a year
y = year

To get the number of days in a specific month, N_m, using the `julian_day` function:

$$N_m = \text{julian\_day}(y, m + 1, 1) - \text{julian\_day}(y, m, 1) \tag{2}$$

where:
N_m = number of days in a month
m = month, (i.e., 1–12)

To get the current day of the year, n, using the `julian_day` function:

$$n = \text{julian\_day}(y, m, i) - \text{julian\_day}(y, 1, 1) + 1 \tag{3}$$

where:
n = day of the year
i = day of the month, (i.e., 1–31)

2.1.1 Vernal equinox

The vernal equinox (i.e., spring or March equinox) falls on 19–21 March (day of the year 79–81). A historical calendar of vernal equinox dates can be found online[2]. While a constant value of 80 may be assumed, the day of the year of the vernal equinox, n_{ve}, can be calculated for a given year (ibid., Ch. 26). The algorithm for this calculation is given in Appendix A.2.

2.2 Evaporative Supply

The instantaneous evaporative supply, S_w, is prescribed as being linearly proportional to the soil moisture, which is defined in terms of relative wetness (instead of absolute moisture content) (Federer 1982):

$$S_w = S_c \, \frac{W_{n-1}}{W_m} \tag{4}$$

where:
S_w = evaporative supply rate, mm·h^{-1}
S_c = maximum rate of evaporation, mm·h^{-1}
W_{n-1} = yesterday's soil moisture content, mm
W_m = soil moisture capacity, mm

The assumed constant values for S_c and W_m are given in Table 1. The cumulative daily supply water, S, is integrated over the number of daylight hours, d_s assuming a sinusoidal curve (ibid., Eq. 18b):

$$\int_{day} S_w = S = d_s \, S_w \tag{5}$$

where:
S = daily evaporative supply, mm
S_w = evaporative supply rate, mm·h^{-1}
d_s = number of daylight hours, h

2.3 Extraterrestrial Solar Radiation Flux

Evaporative demand is calculated based on net radiation flux. To begin, the solar irradiance at the top of the atmosphere, I_o, or extraterrestrial solar radiation flux, is calculated with the following (Duffie and Beckman 2013, Eq. 1.10.2):

$$I_o = I_{sc} \, d_r \, \cos\theta_z \tag{6}$$

where:
I_o = extraterrestrial solar radiation flux, W·m^{-2}
I_{sc} = solar constant, W·m^{-2}
d_r = distance factor, unitless

[2] `http://ns1763.ca/equinox/vern1788-2211.html`

$\cos\theta_z$ = inclination factor, unitless

Note that negative values of I_o represent when the sun is below the horizon and, having no physical meaning, should be set equal to zero.

2.3.1 Solar constant

The solar constant (I_{sc}) has a complex behavior and is subject to temporal variability (Crommelynck and Dewitte 1997), which is caused by the changing distribution of solar brightness features (e.g., sunspots, faculae, and the network) (Krivova et al. 2010). There have been several attempts throughout history to measure the solar constant.

Early attempts made by ground-based observation stations quantified the solar constant to be approximately 1340 W·m^{-2} (Abbot and Fowle 1911) to 1348 W·m^{-2} (Abbot 1914).

In 1978, the first space-borne observations of the solar constant were made after the launch of the Earth Radiation Budget (ERB) satellite. In 1980, the Solar Maximum Mission satellite (SMM) (hosting the ACRIM I sensor) and the Earth Radiation Budget Satellite (ERBS) were launched. Two more satellites were launched, the NOAA9 in 1984 and the NOAA10 in 1986. In 1995, the Solar and Heliospheric Observatory (SOHO) satellite was launched for the continuous observation of the sun (via the VIRGO sensor). Other observations include the HF on the NIMBUS 7 satellite, the SOVA on the EURECA satellite, ACRIM II on the UARS satellite, and ACRIM III on the ACRIM-Sat satellite. The 2003 launch of NASA's Solar Radiation and Climate Experiment (SORCE) satellite with an onboard Total Irradiance Monitor (TIM), provides long-term stable measurements of total solar irradiance with three times the accuracy of previous satellite measurements (Kopp and Lean 2011).

There have been attempts at creating a composite of the various satellite datasets: the PMOD composite (Fröhlich 2006), the ACRIM composite (Willson 1997), and the IRMB composite (Dewitte et al. 2004). The latest composite is based on the average of the three previous composites and scaled to match the SOURCE TIM satellite observations (Kopp and Lean 2011).

The solar constant that is adopted for use in this study is given in Table 1.

2.3.2 Distance factor

The distance factor is the inverse square of the relative distance between the earth and sun, ρ_d:

$$d_r = \left(\frac{1}{\rho_d}\right)^2 \tag{7}$$

where:
ρ_d = relative earth-sun distance, unitless

The relative earth-sun distance is simply (Loutre 2002):

$$\rho_d = \frac{r}{a} \tag{8}$$

where:
r = distance from earth to the sun, km
a = length of the semi-major axis of earth's orbit, km

In geological time, the semi-major axis of earth's orbit does not significantly change (approximate value given in Table 1). In contrast, as the earth travels around the sun, due to the elliptic nature of its orbit, the distance between the earth and sun changes, closest at the perihelion ($r \approx 1.471 \times 10^8$ km) and farthest at the aphelion ($r \approx 1.521 \times 10^8$ km) (Allen 1973). The distance from the earth to the sun can be expressed through the equation of the ellipse (Loutre 2002):

$$r = \frac{a\ \left(1 - e^2\right)}{1 + e\ \cos\nu} \tag{9}$$

where:
e = eccentricity of earth's orbit, unitless
ν = heliocentric longitude relative to the perihelion, radians

A current value of eccentricity is given in Table 1.

It is common that earth's position is given relative to the vernal equinox (not the perihelion). The relationship between the two measures of heliocentric longitude is given by:

$$\nu = \lambda - \tilde{\omega} \tag{10}$$

where:
λ = heliocentric longitude relative to the vernal equinox, radians
$\tilde{\omega}$ = longitude of the perihelion, radians

To approximate the distance factor, some researchers have simplified 7 based on two assumptions. The first assumption is that the eccentricity is near zero and therefore negligible. In the present day, earth's orbital eccentricity is roughly 0.0167 and is decreasing at a rate of approximately 0.00004 per century[3]. This allows for higher order terms to be ignored.

The second assumption is that the earth travels around the sun at a constant angular velocity. In reality, as the earth approaches the sun during

[3] http://mb-soft.com/public3/equatime.html

the perihelion (currently during the first week of January), earth's orbital angular velocity increases and as earth approaches the aphelion (currently during the first week of July), earth's orbital angular velocity decreases. By assuming a constant angular velocity, earth's longitude can be approximated by the day fraction of the year.

Based on these two assumptions, the distance factor can be approximated by (Klein 1977):

$$d_r = 1 + 2e\ \cos\left(\frac{2\pi\ n}{N}\right) \tag{11}$$

The difference between Eq. 11 and Eq. 7, with ν mapped to the day of the year using the simplified Kepler method, is about 0.16% with a maximum error of about 0.30% during the latter half of the year (see Figure 1). This larger discrepancy is due to the slowing of earth's orbital velocity as it travels away from the sun, which is not modeled in Eq. 11.

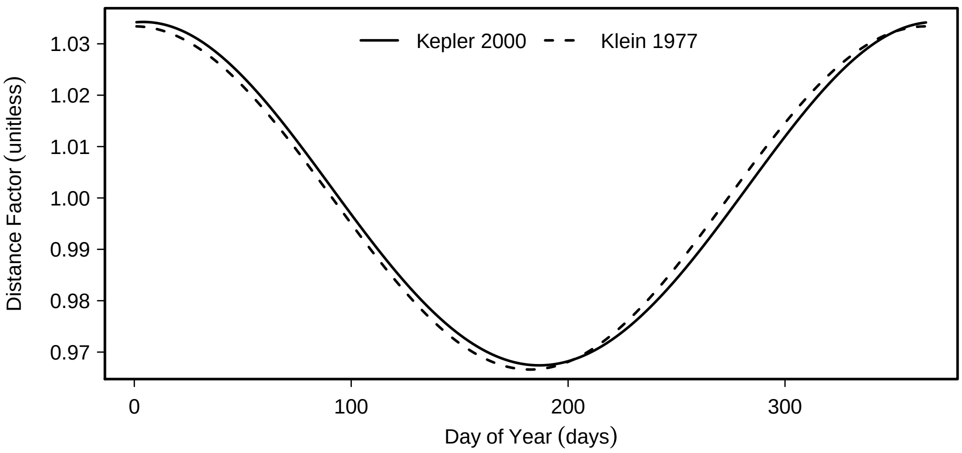

Figure 1: Comparison between actual distance factor, d_r, using the simplified Kepler method for 2000 CE, and the approximation method by Klein (1977).

2.3.3 Inclination factor

The inclination factor, $\cos\theta_z$, attenuates the incident solar radiation perpendicular to earth's surface to account for earth's tilted surface at different latitudes. The sun's elevation angle above the horizon is measured by the zenith angle (θ_z). A general expression relating the angle of incidence (θ), to other angles that describe the geometric relationship between a plane on the surface of the earth and an incoming beam of solar radiation is given by (Duffie and Beckman 2013, Eq. 1.6.2):

$$
\begin{aligned}
\cos\theta = &\sin\delta\ \sin\phi\ \cos\beta \\
&- \sin\delta\ \cos\phi\ \sin\beta\ \cos\gamma \\
&+ \cos\delta\ \cos\phi\ \cos\beta\ \cos h \\
&+ \cos\delta\ \sin\phi\ \sin\beta\ \cos\gamma\ \cos h \\
&+ \cos\delta\ \sin\beta\ \sin\gamma\ \sin h
\end{aligned} \tag{12}
$$

where:
δ = declination angle, radians
ϕ = latitude, radians
β = slope, radians
γ = surface azimuth angle, radians
h = hour angle, radians

For a horizontal surface (i.e., $\beta = 0$), the angle of incidence below the zenith (i.e., $0° \leq \theta_z \leq 90°$) is given by (Duffie and Beckman 2013; Loutre 2002; Wetherald and Manabe 1972):

$$\cos\theta_z = \sin\delta\ \sin\phi + \cos\delta\ \cos\phi\ \cos h \tag{13}$$

For a given latitude, ϕ, there are two terms that need to be computed for the calculation of the inclination factor: the declination angle (δ) and the hour angle (h).

2.3.4 Declination angle

The declination angle is defined as the angular position between the sun at solar noon and the earth's equator (ranging from -23.45° during the winter solstice to 23.45° during the summer solstice). The following calculation method for δ is for any given time of year (Loutre 2002; Woolf 1968):

$$\delta = \arcsin\left(\sin\lambda\ \sin\epsilon\right) \tag{14}$$

where:
λ = heliocentric longitude relative to the vernal equinox, radians
ϵ = obliquity of earth's axis, radians

Obliquity, or the off-vertical axial tilt around which the earth rotates, is the third time-varying orbital parameter (the other two being e and $\tilde{\omega}$). The obliquity angle varies between 22.1° and 24.5° with a periodicity of about 41000 years (Berger 1977; Hays et al. 1976). A value for the 2000 CE epoch is given in Table 1.

Approximations of the declination angle have been made based on the day of the year instead of earth's longitude (similar to the distance factor approximation). The following assumes that earth's orbit is a perfect circle:

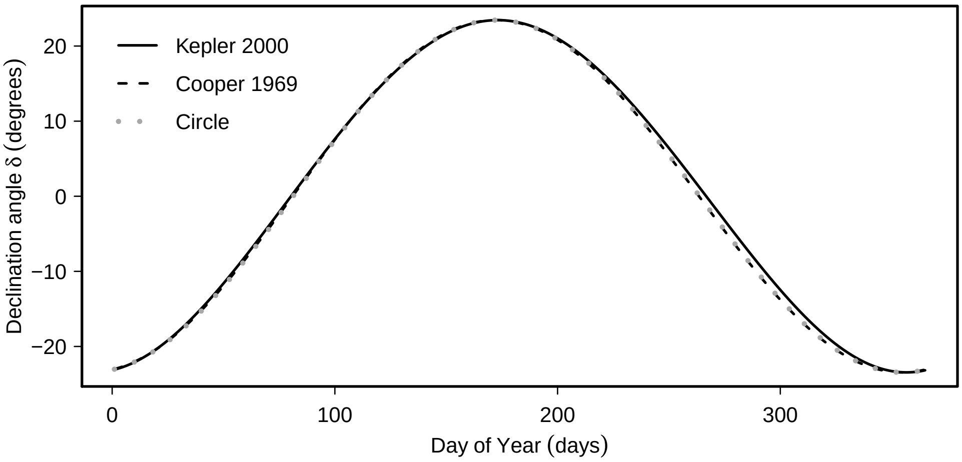

Figure 2: Comparison between actual declination angle, δ, using the simplified Kepler method for 2000 CE, the approximation method by Cooper (1969), and the perfect circle approximation.

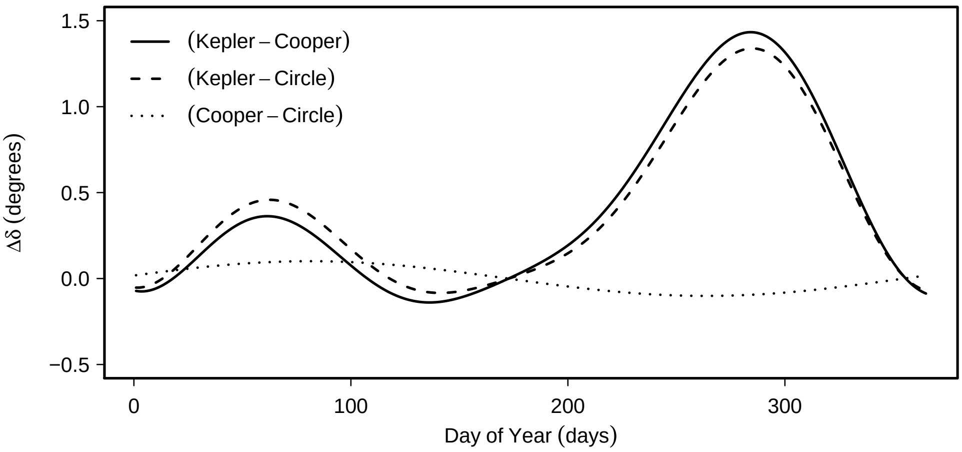

Figure 3: Differences between actual declination angle, δ, using the simplified Kepler method for 2000 CE, the approximation method by Cooper (1969), and the perfect circle approximation.

$$\delta = -\epsilon \cos\left(\frac{2\pi\,(n+10)}{N}\right) \tag{15}$$

Cooper 1969 presents a similar approximation to Eq. 15 as:

$$\delta = \epsilon \sin\left(\frac{2\pi\,(n+284)}{N}\right) \tag{16}$$

The two approximations (i.e., Eq. 15 and Eq. 16) are almost identical through the trigonometric identity: $-\cos x = \sin(x - \pi/2)$ (i.e., equivalence occurs at a value of 283.75 in Eq. 16).

Spencer 1971 derived a third approximation to δ based on a Fourier analysis of data presented in the Nautical Almanac (1950 C.E. epoch), given in units of radians:

$$\begin{aligned}\delta =& 0.006918 - 0.399912\ \cos B + 0.070257\ \sin B - \\ & 0.006758\ \cos 2B + 0.000907\ \sin 2B - \\ & 0.002697\ \cos 3B + 0.00148\ \sin 3B\end{aligned} \tag{17}$$

where $B = 2\pi\ (n-1)\ N^{-1}$.

A comparison of δ as calculated by Eq. 14, Eq. 15, and Eq. 16 is given in Figure 2. There is a slight difference between the results given by Eq. 15 and Eq. 16 due to the slight inequality in the expressions. Similar to Figure 1, the largest difference between the approximation methods and that calculated by Eq. 14 happens in the latter half of the year (see Figure 3).

2.3.5 Hour angle

The hour angle, h, is the angular displacement of the sun east or west of the local meridian. It is measured ranging from -180° to 180° with 0° occurring at solar noon. An approximation of the hour angle is given as follows (Cooper 1969):

$$h = \frac{2\pi}{24}\,(d_s - t_r) \tag{18}$$

where:
d_s = number of daylight hours, h
t_r = number of hours past sunrise, h

The approximation made in Eq. 18 is based on the average rate of earth's spin (i.e., 360° per 24 hr). Knowledge of the sunrise hour is necessary for computing Eq. 18.

A more precise method of calculating h follows (Stine and Geyer 2001, Eq. 3.1):

$$h = \frac{2\pi}{24}\,(t_s - 12) \tag{19}$$

where:
t_s = solar time, h

Solar time is the apparent angular motion of the sun across the sky with solar noon representing the time when the sun crosses the local meridian of the observer. The conversion between local clock time (LCT) and solar time (t_s) depends on the physical observation location, the day of the year, and the time zone of the location. The conversion equation takes the form of (Stine and Geyer 2001, Eq. 3.5):

$$t_s = LCT + \frac{EOT}{60} - LC - DS \tag{20}$$

where:
LCT = local clock time, h
EOT = equation of time, min
LC = longitude correction factor, h
DS = daylight savings correction factor, h

The equation of time (EOT) is the measure of difference between the mean solar time and the true solar time. Due to the seasonal changes which account for the mean solar time, the actual solar time can be as great at ± 17 min from the mean (ibid.). An approximation of EOT (in minutes) is given by (Woolf 1968, Eq. 1.6):

$$\begin{aligned} EOT = 60 \times (&0.004289 \ \cos B \\ &- 0.12357 \ \sin B \\ &- 0.060783 \ \cos 2B \\ &- 0.153809 \ \sin 2B) \end{aligned} \tag{21}$$

where:
$B = 2\pi \, (n-1) \, N^{-1}$

An updated calculation of EOT was developed (Spencer 1971) and corrected (Oglesby 1998), accurate to within 35 seconds, and is presented in units of minutes (Iqbal 1983):

$$\begin{aligned} EOT = \frac{1440}{2\pi} \times (&7.5 \times 10^{-6} \\ &+ 1.868 \times 10^{-3} \ \cos B \\ &- 3.2077 \times 10^{-2} \ \sin B \\ &- 1.4615 \times 10^{-2} \ \cos 2B \\ &- 4.0849 \times 10^{-2} \ \sin 2B) \end{aligned} \tag{22}$$

where the factor ($1440/(2\pi) \approx 229.18$) converts radians into minutes based on the 24 hours required for the earth to make a full rotation (i.e., 2π radians). Figure 4 shows a comparison between EOT as calculated using Eq. 21 and Eq. 22. The difference between these two methods varies between

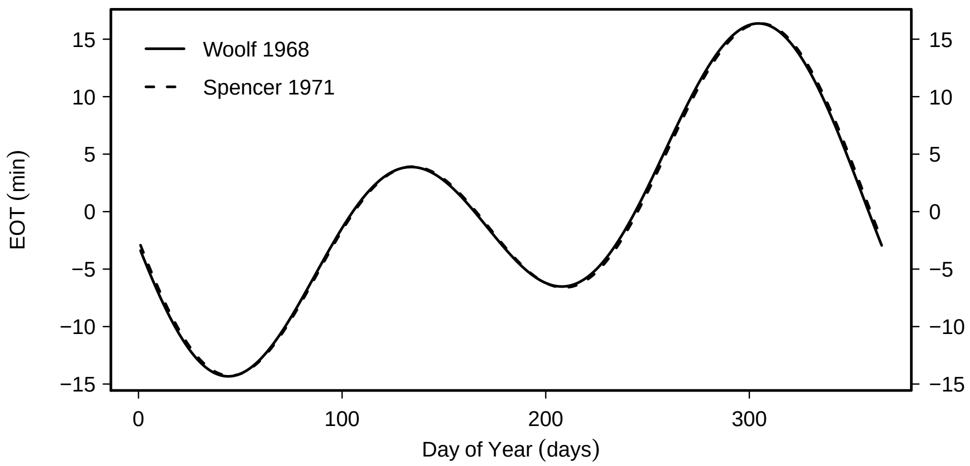

Figure 4: Comparison between EOT as calculated by Woolf (1968) and Spencer (1971).

approximately ± 0.45 minutes (i.e., ± 27 seconds).

The longitude correction factor (LC) makes the appropriate adjustment for the local time zone difference from the UTM/GMT based on the rotational speed of the Earth (2π radians in 24 hours) and is given by (Stine and Geyer 2001):

$$LC = \left(\frac{\pi}{12} \, TZ_h - \theta_{lon} \right) \, \frac{12}{\pi} \tag{23}$$

where:
TZ_h = number of time zones away from UTC, h
θ_{lon} = longitude of observation, radians

The daylight savings time correction factor, DS, corrects local time when summer time is in (i.e., $DS = 1$) and is ignored otherwise.

2.3.6 True longitude

Earth's true longitude, λ, (i.e., the heliocentric longitude relative to the vernal equinox) can be estimated for a given day, n. A simple estimation is given assuming a constant orbital velocity by (Woolf 1968):

$$\begin{aligned}\lambda^* =& 279.9348 + B^* \\ &+ 1.914827 \, \sin^* B^* - 0.079525 \, \cos^* B^* \\ &+ 0.019938 \, \sin^* 2B^* - 0.00162 \, \cos^* 2B^*\end{aligned} \tag{24}$$

where:
$\lambda^* = \lambda$ (in degrees)
$B^* = 360\,(n-1)\ N^{-1}$ (in degrees)

Note that $\sin^*$ and $\cos^*$ indicate the sine and cosine of angles in degrees. This is to account for B^* in Eq. 24, which must be in units of degrees.

Berger 1978 presents an algorithm for computing the true longitude for a given day, n, based on a mean earth orbit. The method first computes a mean longitude, λ_{m0}, for the day of the vernal equinox (assumed 21 March, $n = 80$ for a 365-day year):

$$\begin{aligned}\lambda_{m0} =& 2\left(\frac{e}{2}+\frac{e^3}{8}\right)(1+\beta)\ \sin\tilde{\omega} - \\ & \frac{e^2}{2}\left(\frac{1}{2}+\beta\right)\sin 2\tilde{\omega} + \\ & \frac{e^3}{4}\left(\frac{1}{3}+\beta\right)\ \sin 3\tilde{\omega}\end{aligned} \tag{25}$$

where $\beta = \sqrt{1-e^2}$. The mean longitude for a given day, λ_m, is then calculated assuming a constant orbital speed:

$$\lambda_m = \lambda_{m0} + \frac{2\pi\,(n-80)}{N} \tag{26}$$

and the true longitude is then back-calculated from the mean longitude:

$$\lambda = \lambda_m + \left(2e - \frac{1}{4}e^3\right)\ \sin\nu_m + \frac{5}{4}e^2\ \sin 2\nu_m + \frac{13}{12}e^3\ \sin 3\nu_m \tag{27}$$

where $\nu_m = \lambda_m - \tilde{\omega}$.

A third approximation to λ is derived from Kepler's laws of planetary motion. The derivation begins with the formulaic expression of Kepler's second law of planetary motion:

> *"A line joining a planet and the Sun sweeps out equal areas during equal intervals of time."*— Kepler's Second Law

$$\frac{dA_s}{dt} = \frac{r^2}{2}\frac{d\nu}{dt} \tag{28}$$

where:
A_s = sweep area of the ellipse, km^2
t = time during which a planet has traveled some distance, days
ν = heliocentric longitude relative to the perihelion, radians
r = distance from a planet to the sun, km

Integrating the left-hand side of Eq. 28 results in the area of an ellipse, such that:

$$\frac{2\pi\, a\, b}{N} = r^2\, \frac{d\nu}{dt} \tag{29}$$

where:
a = length of the semi-major axis of earth's orbit, km
b = length of the semi-minor axis of earth's orbit, km
N = earth's orbital period, days

To keep Eq. 29 in terms of the semi-major axis, a, and eccentricity, e, the equation for eccentricity can be solve for b:

$$b = a\,\sqrt{1 - e^2} \tag{30}$$

The angular velocity, $d\nu/dt$, can now be solved by replacing Eq. 30 into Eq. 29:

$$\frac{d\nu}{dt} = \left(\frac{a}{r}\right)^2\, \frac{2\pi\sqrt{1-e^2}}{N} \tag{31}$$

Substituting Eq. 9 into Eq. 31 yields:

$$\frac{d\nu}{dt} = \frac{2\pi}{N}\, \frac{(1 + e\, \cos\nu)^2}{(1-e^2)^{1.5}} \tag{32}$$

A methodology for solving the heliocentric longitude for a given time, t, follows (Kutzbach and Gallimore 1988):

$$dt = \frac{N\,\left(1-e^2\right)^{1.5}}{2\pi}\, (1 + e\, \cos\nu)^{-2}\, d\nu \tag{33}$$

Integrating both sides results in:

$$t = \frac{N\,\left(1-e^2\right)^{1.5}}{2\pi} \int (1 + e\, \cos\nu)^{-2}\, d\nu \tag{34}$$

The non-trivial integrand on the right-hand side of Eq. 34 has a long and complicated integral, which was solved using the Maxima computer algebra system[4].

[4] http://maxima.sourceforge.net/

$$
\begin{aligned}
&\int (1 + e\ \cos\nu)^{-2}\, d\nu = \\
&\quad 2\,\frac{\arctan\left(\frac{(2e-2)\ \sin\nu}{2\sqrt{1-e^2}\ (\cos\nu+1)}\right)}{\sqrt{1-e^2}\ (e^2-1)} + \\
&\quad -2\,\frac{e\ \sin\nu}{(\cos\nu+1)\ \left(\frac{(e^3-e^2-e+1)\ \sin^2\nu}{(\cos\nu+1)^2} - e^3 - e^2 + e + 1\right)}
\end{aligned} \tag{35}
$$

An approximation to this integral can be made assuming that eccentricity is small, such that higher powers of eccentricity can be ignored. Following the elimination of high-powered eccentricity terms:

$$
\begin{aligned}
&\int (1 + e\ \cos\nu)^{-2}\, d\nu \approx \\
&\quad -2\ \arctan\left[\frac{(e-1)\ \sin\nu}{\cos\nu+1}\right] + \\
&\quad -2\,\frac{e\ \sin\nu\,(\cos\nu+1)}{(1-e)\ \sin^2\nu + (1+e)\ (\cos\nu+1)^2}
\end{aligned} \tag{36}
$$

Now, assume that eccentricity in the quantities $(e-1)$, $(1-e)$, and $(1+e)$ is negligible.

$$
\begin{aligned}
&\int (1 + e\ \cos\nu)^{-2}\, d\nu \approx \\
&\quad 2\ \arctan\left(\frac{\sin\nu}{\cos\nu+1}\right) - \frac{2e\ \sin\nu\,(\cos\nu+1)}{\sin^2\nu + \cos^2\nu + 2\cos\nu + 1}
\end{aligned} \tag{37}
$$

Finally, simplifying the second term leads to:

$$
\int (1 + e\ \cos\nu)^{-2}\, d\nu \approx 2\ \arctan\left(\frac{\sin\nu}{\cos\nu+1}\right) - e\ \sin\nu \tag{38}
$$

A comparison between the full derivative (i.e., Eq. 35) and the simplification (i.e., Eq. 38) revealed a discrepancy in the magnitude of the second term in Eq. 38 by a factor of two. Following this addition, substituting it back into Eq. 34, and assuming that $(1-e^2)^{1.5} \approx 1$, the equation for the simplified Kepler mapping is:

$$
t = \frac{N}{\pi}\ \left[\arctan\left(\frac{\sin\nu}{\cos\nu+1}\right) - e\ \sin\nu\right] \tag{39}
$$

Figure 5 shows the difference between Eq. 34 and Eq. 39 (full integral versus the simplified integral). The magnitude of the difference between the

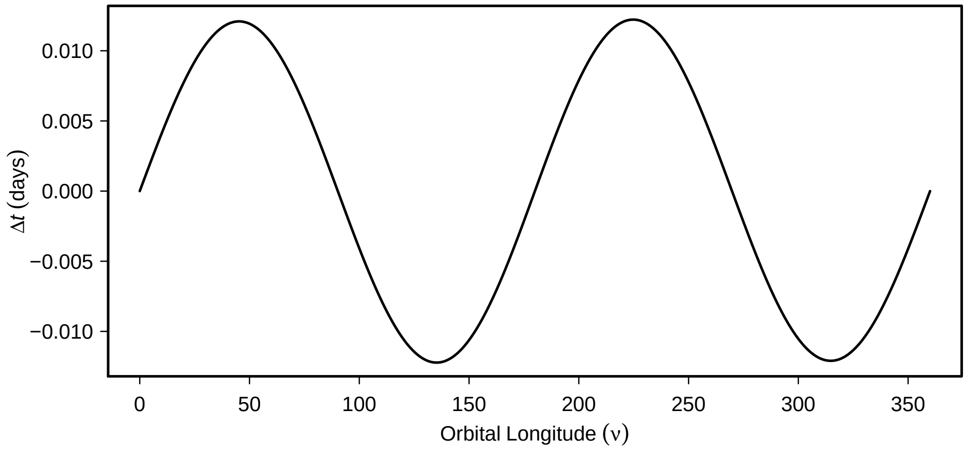

Figure 5: Difference between the full integral and simplified integral solutions of t for a given ν.

two methods is approximately 35.2 minutes, which is more than reasonable given the amount of simplification that was made.

To complete the mapping, the calendar days of a particular year need to be associated with t in Eq. 39. This is accomplished through the definition of λ (i.e., Eq. 10). For a known $\tilde{\omega}$, ν at the vernal equinox can be solved by setting $\lambda = 0$. First find the number of days it takes the earth to travel from the perihelion ($\nu = 0$) to the vernal equinox ($\nu_{ve} = 360 - \tilde{\omega}$) by solving Eq. 39. Next, either solve for specific day of the year, n, on which the vernal equinox falls (i.e., Appendix A.2) or assume a constant day of the year (e.g., $n_{ve} = 80$). The difference between n_{ve} and $t(\nu_{ve})$ corresponds to the calendar day at the perihelion.

For example, assuming the current value of $\tilde{\omega} = 283°$, then $t(360 - \tilde{\omega}) =$ 76.2 days. The difference between a constant $n_{ve} = 80$ and t at the vernal equinox is 3.8 days. This is reasonable given that the date of the perihelion is typically within the first week of January.

In order to get λ for a given n, solve Eq. 39 for each 1° of ν. Next, find the value of t that is as close to, but not greater than n. Then, move the earth forward in space equivalent to the orbital velocity at position $\nu(t)$ multiplied by the difference in time (i.e., $n - t$) using Eq. 32. Lastly, use Eq. 10 to solve for $\lambda(n)$, making certain to keep values of $\lambda \leq 360°$.

2.4 Daily Extraterrestrial Solar Radiation

Often, it is necessary to calculate the total daily solar irradiance (i.e., the integration of instantaneous solar irradiance over the course of the day). This can be analytically done by integrating the instantaneous extraterrestrial solar radiation curve, defined by Eq. 6 (see §2.3), over the daylight hours.

Using the definition of the hour angle, h (see §2.3.5), the sunset angle, h_s, can be calculated when $I_o = 0$. Using the inclination factor for horizontal surfaces (i.e., Eq. 13) the equation for instantaneous solar radiation is:

$$I_o = I_{sc}\, d_r\, \left(\sin\delta\, \sin\phi + \cos\delta\, \cos\phi\, \cos h\right) \tag{40}$$

Setting Eq. 40 equal to zero and solving for the sunset hour angle:

$$h_s = \arccos\left(\frac{-\sin\delta\, \sin\phi}{\cos\delta\, \cos\phi}\right) = \arccos\left(-\tan\delta\, \tan\phi\right) \tag{41}$$

where:
h_s = sunset hour angle, radians
δ = declination angle, radians
ϕ = latitude, radians

Special care needs to be made when $\tan\delta\, \tan\phi \geq 1$ (i.e., polar day, no sunset, $h_s = \pi$) and when $\tan\delta\, \tan\phi \leq -1$ (i.e., polar night, no sunrise, $h_s = 0$).

The daylight hours are calculated from sunrise, $-h_s$, to sunset, h_s. To calculate the daylight hours, d_s, double the sunset hour (to accommodate for the time between sunrise and solar noon) and convert the angle to hours, based on the rate of earth's rotation (i.e., 24 hours per 2π radians):

$$d_s = \frac{24\, h_s}{\pi} \tag{42}$$

where:
d_s = hours of daylight, h
h_s = sunset hour angle, radians

The daily integral of solar radiation can now be solved by integrating Eq. 40 from solar noon, h_o, to sunset, h_s, assuming that the angles related to earth's orbital position are constant for the whole day (see Figure 6):

$$\int_0^{h_s} I_o = I_{sc}\, d_r\, \left(\sin\delta\, \sin\phi\, h_s + \cos\delta\, \cos\phi\, \sin h_s\right) \tag{43}$$

The total daily solar radiation, H_o, is found by doubling the quantity in Eq. 43 (again to account for the morning half of the daily radiation curve) and converting the units integrated over from radians to seconds (i.e., 86400 seconds per day):

$$H_o = \frac{86400}{\pi}\, I_{sc}\, d_r\, \left(\sin\delta\, \sin\phi\, h_s + \cos\delta\, \cos\phi\, \sin h_s\right) \tag{44}$$

where:
H_o = daily total extraterrestrial solar radiation, J·m^{-2}

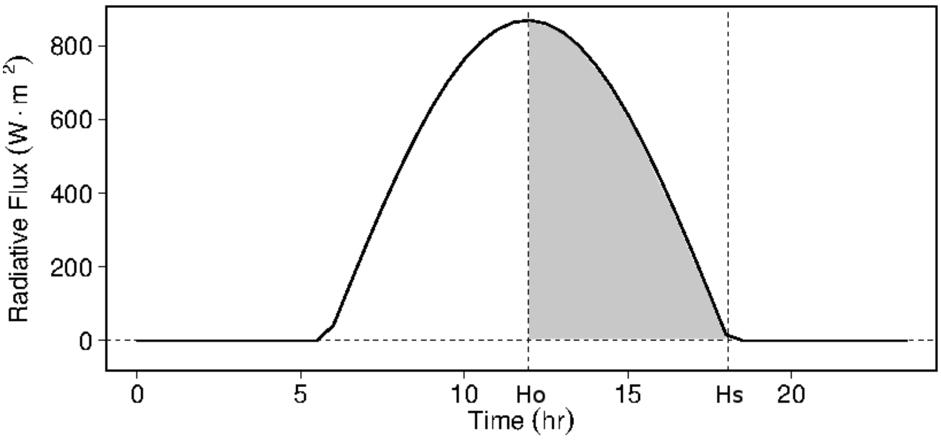

Figure 6: Half-day integral of I_o from solar noon, h_o, to sunset, h_s (shaded area).

2.5 Net Radiation Flux

The net radiation is defined as (Linacre 1968, Eq. 4):

$$I_N = I_{SW} - I_{LW} \tag{45}$$

where:
I_N = net radiation, W·m^{-2}
I_{SW} = net shortwave downwelling solar radiation, W·m^{-2}
I_{LW} = net longwave radiation, W·m^{-2}

Due to the lack of observations of radiation quantities on the global scale, net shortwave and longwave radiation must be modeled.

2.5.1 Shortwave radiation flux

Net incoming shortwave solar radiation, I_{SW}, can be modeled after the extraterrestrial solar radiation, I_o (see §2.3 by accounting for the amount of radiation that is reflected:

$$I_{SW} = (1 - \beta_{sw})\ I_{S\downarrow} \tag{46}$$

where:
I_{SW} = net shortwave solar radiation flux, W·m^{-2}
$I_{S\downarrow}$ = incident shortwave solar radiation flux, W·m^{-2}
β_{sw} = shortwave albedo, unitless

A value for the shortwave albedo, β_{sw}, is given in Table 1. The incident shortwave solar radiation can be expressed as the atmospheric transmittivity, τ, multiplied by I_o:

$$I_{S\downarrow} = \tau \, I_o \tag{47}$$

where:
$I_{S\downarrow}$ = incident shortwave solar radiation flux, W·m^{-2}
I_o = extraterrestrial solar radiation flux, W·m^{-2}
τ = atmospheric transmittivity, unitless

Atmospheric transmittivity may be modeled as a function of sunshine hours and elevation. The presence of clouds (i.e., fewer sunshine hours) reduces the amount of shortwave radiation that reaches the surface. Similarly, at higher elevations, there is less atmosphere through which the shortwave radiation must travel, thereby increasing the amount of radiation reaching the surface. Assuming a mean sea-level transmittivity level follows the Ångstrom-Prescott model:

$$\tau_o = c + d \, S_f \tag{48}$$

where:
τ_o = mean sea-level transmittivity, unitless
c = minimum transmittivity for cloudy skies, unitless
d = angular coefficient of transmittivity, unitless
S_f = fraction of daily bright sunshine hours ($0 \leq S_f \leq 1$)

Empirical values for c and d are given in Table 1. To accommodate the increase in transmittivity with elevation, τ_o can be corrected with a based on the regression of Beer's radiation extinction function below 3000 m with an average sun angle of 45° (Allen 1996):

$$\tau = \tau_o \, \left(1 + 2.67 \times 10^{-5} \, z\right) \tag{49}$$

where:
τ = elevation-corrected atmospheric transmittivity, unitless
z = elevation, m

2.5.2 Longwave radiation flux

The net outgoing longwave radiation (i.e., thermal radiation) is comprised of the difference between the surface (upward) and the atmospheric (downward) radiant heat multiplied by a cloudiness adjustment factor, which can be approximated based on mean daily air temperature (Linacre 1968):

$$
\begin{aligned}
I_{LW} &= (I_{L\uparrow} - I_{L\downarrow})\,(b + (1-b)\,S_f) \\
&\approx (b + (1-b)\,S_f)\,(A - T_{air})
\end{aligned}
\tag{50}
$$

where:
I_{LW} = net longwave radiation, W·m^{-2}
$I_{L\uparrow}$ = longwave upward radiation flux, W·m^{-2}
$I_{L\downarrow}$ = longwave clear-sky downward radiation flux, W·m^{-2}
b = empirical constant
S_f = fraction of daily bright sunshine hours
A = empirical constant
T_{air} = mean daily air temperature, °C

Values for A and b are given in Table 1. The upward flux of longwave radiation may be modeled assuming a constant emissivity (e.g., under well-watered conditions) (ibid., Eq. 21):

$$
I_{L\uparrow} = \sigma_{sb}\ (T_{air} + 273.15)^4 \tag{51}
$$

where:
$I_{L\uparrow}$ = longwave upward radiation flux, W·m^{-2}
σ_{sb} = Stefan-Boltzman constant, W·m^{-2}·K^{-4}
T_{air} = mean daily air temperature, °C

The downward clear-sky atmospheric longwave radiation is given by (ibid., Eq. 20):

$$
I_{L\downarrow} = 1.19\,\sigma_{sb}\ (T_{air} + 273.15)^4 - 171 \tag{52}
$$

where:
$I_{L\downarrow}$ = longwave clear-sky downward radiation flux, W·m^{-2}
σ_{sb} = Stefan-Boltzman constant, W·m^{-2}·K^{-4}
T_{air} = mean daily air temperature, °C

2.6 Daily Daytime Net Radiation

The daily integration of the net radiation curve requires the definition of the cross-over hour angle, h_n, which occurs when $I_N = 0$. From Eq. 45, substituting Eq. 46 and Eq. 47 for the shortwave radiation flux and assuming I_o for a horizontal surface:

$$
I_N = (1 - \beta_{sw})\ \tau\ I_{sc}\, d_r\ (\sin\delta\ \sin\phi + \cos\delta\ \cos\phi\ \cos h) - I_{LW} \tag{53}
$$

Setting $I_N = 0$ and solving Eq. 53 for the hour angle:

$$h_n = \arccos\left[\frac{I_{LW}}{(1-\beta_{sw})\ \tau\, I_{sc}\, d_r\ \cos\delta\ \cos\phi} - \tan\delta\ \tan\phi\right] \tag{54}$$

Eq. 54 may be simplified by making the following substitutions: $r_u = \sin\delta\ \sin\phi$, $r_v = \cos\delta\ \cos\phi$, $r_w = (1-\beta_{sw})\ \tau\, I_{sc}\, d_r$, such that Eq. 54 may be rewritten as:

$$h_n = \arccos\left(\frac{I_{LW} - r_w\, r_u}{r_w\, r_v}\right) \tag{55}$$

where:

h_n = net radiation flux cross-over hour angle, radians
I_{LW} = net longwave radiation flux, W·m^{-2}
$r_u = \sin\delta\ \sin\phi$, unitless
$r_v = \cos\delta\ \cos\phi$, unitless
$r_w = (1-\beta_{sw})\ \tau\, I_{sc}\, d_r$, W·m^{-2}

Special care needs to be made when $(I_{LW} - r_w\, r_u)/(r_w\, r_v) \geq 1$ (i.e., net radiation always less than zero, $h_n = 0$) and when $(I_{LW} - r_w r_u)/(r_w r_v) \leq -1$ (i.e., net radiation always greater than zero, $h_n = \pi$).

The half-day integral of net radiation can now be solved by integrating Eq. 53 from solar noon to h_n (see Figure 7):

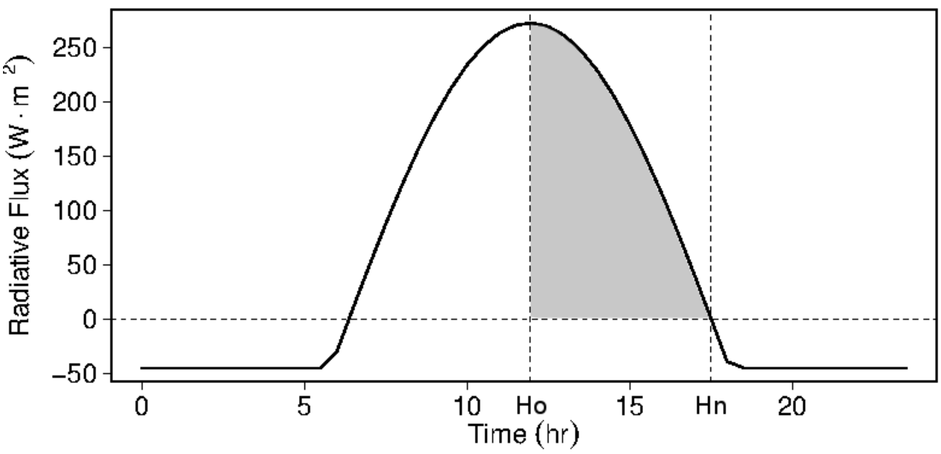

Figure 7: Half-day integral of H_N from solar noon, h_o, to cross-over hour angle, h_n (shaded area).

$$\int_0^{h_n} I_N = r_w\ (r_u\, h_n + r_v\ \sin h_n) - I_{LW}\, h_n \tag{56}$$

The total daily net radiation, H_N, is found by doubling the quantity in Eq. 56 (i.e., twice the half-day amount) and converting the units integrated over from radians to seconds:

$$H_N = \frac{86400}{\pi} \left[(r_w\, r_u - I_{LW})\; h_n + r_w\, r_v\, \sin h_n \right] \tag{57}$$

where:

H_N = daily daytime net radiation, J·m^{-2}
I_{LW} = net longwave radiation flux, W·m^{-2}
h_n = net radiation flux cross-over hour angle, radians
$r_u = \sin\delta\, \sin\phi$, unitless
$r_v = \cos\delta\, \cos\phi$, unitless
$r_w = (1 - \beta_{sw})\; \tau\, I_{sc}\, d_r$, W·m^{-2}

2.7 Daily Nighttime Net Radiation

Some quantities, such as condensation, occur during the nighttime hours and may be modeled as a function of total nighttime net radiation. By utilizing the same methodology used for daily extraterrestrial solar radiation (§2.4) and daily net radiation (§2.6), total nighttime net radiation may be calculated as twice the half-day integral.

The half-day integral for the nighttime net radiation consists of two parts: the I_N curve from h_n to h_s and the I_{LW} curve from h_s to solar midnight, h_p (see Figure 8).

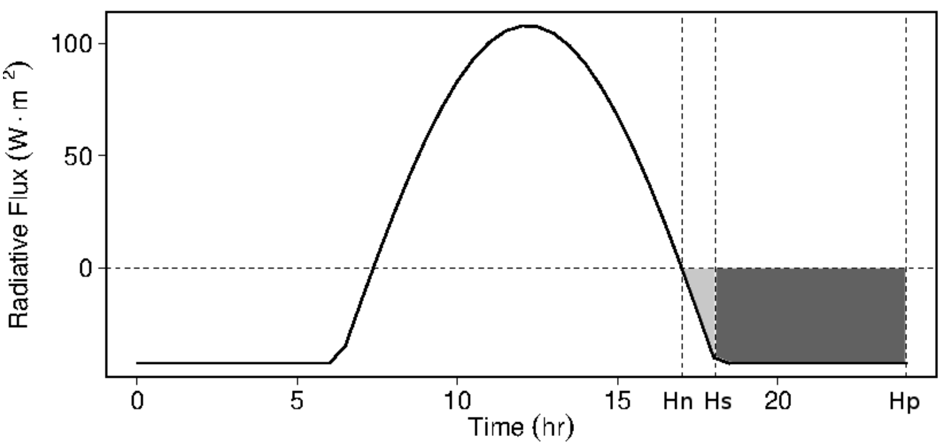

Figure 8: Half-day integral of H_N^* from the cross-over hour, h_n, to sunset, h_s (light shaded area) and from sunset to solar midnight, h_p (dark shaded area).

$$\int_{h_n}^{h_p} I_N = \int_{h_n}^{h_s} I_N + \int_{h_s}^{\pi} I_{LW} \tag{58}$$

Integrating Eq. 58 and using the same variable substitutions described in §2.6:

$$\begin{aligned}\int_{h_n}^{h_p} I_N =& r_w\ \left[r_u\left(h_s - h_n\right) + r_v\left(\sin h_s - \sin h_n\right)\right] \\ &+ I_{LW}\ \left(\pi - 2\,h_s + h_n\right)\end{aligned} \tag{59}$$

The total nightly net radiation, H_N^* is found by doubling the integral of Eq. 58 and converting the units integrated over from radians to seconds:

$$\begin{aligned}H_N^* = \frac{86400}{\pi}\ &\left[r_w\, r_u\left(h_s - h_n\right)\right. \\ &+ r_w\, r_v\left(\sin h_s - \sin h_n\right) \\ &\left.+ I_{LW}\ \left(\pi - 2\,h_s + h_n\right)\right]\end{aligned} \tag{60}$$

where:
H_N^* = daily nighttime net radiation, J·m^{-2}
I_{LW} = net longwave radiation flux, W·m^{-2}
h_n = net radiation flux cross-over hour angle, radians
h_s = sunset hour angle, radians
$r_u = \sin\delta\ \sin\phi$, unitless
$r_v = \cos\delta\ \cos\phi$, unitless
$r_w = (1-\beta)\ \tau\ I_{sc}\, d_r$, W·m^{-2}

Note that the integral is negative (make positive by taking the absolute value).

2.8 Daily Photosynthetic Photon Flux Density

To calculate the daily total photosynthetic photon flux density (PPFD), Q_n, first convert the daily total extraterrestrial solar radiation, H_o (i.e., Eq. 44), to daily total net shortwave radiation (i.e., Eq. 46) based on visible light albedo, then convert shortwave radiation flux to moles of photons using the fFEC conversion factor:

$$Q_n = 1 \times 10^{-6}\ \text{fFEC}\ \left(1 - \beta_{vis}\right)\ \tau\ H_o \tag{61}$$

where:
Q_n = daily photosynthetic photon flux density, mol·m^{-2}
fFEC = from-flux-to-energy conversion, μmol·J^{-1}

β_{vis} = visible light albedo, unitless
τ = atmospheric transmittivity, unitless
H_o = daily extraterrestrial solar radiation, J·m^{-2}

The 1×10^{-6} factor is to convert micro-moles to moles.

2.9 Water–Energy Conversion Factor

To relate radiative energy to evapotranspiration, a conversion factor between volume of water and its associated energy is necessary. The energy conversion factor for water depends on the ambient temperature and pressure. The conversion factor may be written as:

$$E_{con} = \frac{s}{L_v \, \rho_w \, (s + \gamma)} \tag{62}$$

where:
E_{con} = water to energy conversion factor, m^3·J^{-1}
s = slope of saturation vapor pressure temperature curve, Pa·K^{-1}
L_v = latent heat of vaporization of water, J·kg^{-1}
ρ_w = density of water, kg·m^{-3}
γ = psychrometric constant, Pa·°C^{-1}

While standard values may be associated with some of these variables (e.g., $L_v \approx 2.5 \times 10^6$ J·kg^{-1}; $\rho_w \approx 1000$ kg·m^{-3}; $\gamma \approx 65$ Pa·°C^{-1}), their associated dependencies on temperature and pressure are given in the subsections below.

In conditions where atmospheric pressure data are not readily available, the barometric formula may be used to derive the atmospheric pressure based on the elevation above sea level, z.

2.9.1 Barometric Formula

The barometric formula for elevation-dependent atmospheric pressure can be calculated by (Allen et al. 1998):

$$P_{atm} = P_o \left(1 - \frac{L\, z}{T_o}\right)^{\frac{g\, M_a}{R\, L}} \tag{63}$$

where:
P_{atm} = atmospheric pressure, Pa
P_o = base pressure, Pa
T_o = base temperature, K
L = temperature lapse rate, K·m^{-1}
z = elevation, m
g = gravitational acceleration, m·s^{-2}

M_a = molecular weight of dry air, kg·mol^{-1}
R = universal gas constant, J·mol^{-1}·K-1

Values for P_o, T_o, L, g, M_a, and R are available in Table 1.

2.9.2 Slope of saturation pressure temperature curve

The slope of the saturation vapor pressure versus temperature curve, s, at a given temperature is given by (Allen et al. 1998, Eq. 13):

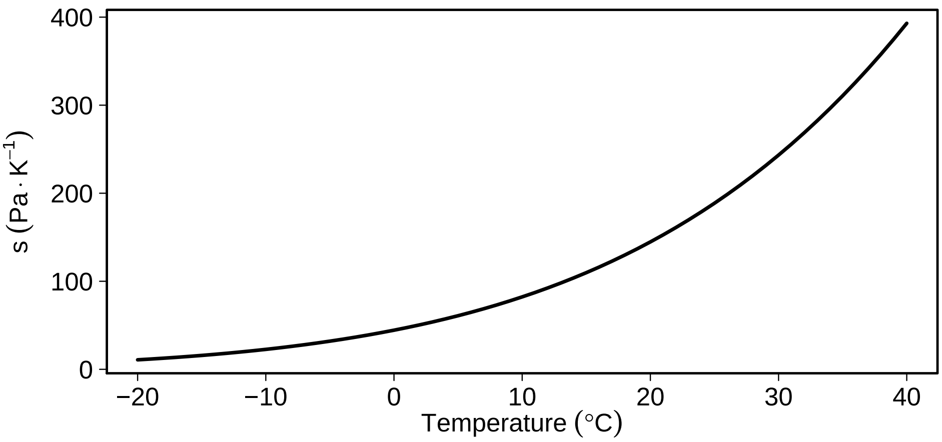

Figure 9: The slope of the saturation vapor pressure temperature curve at temperatures from -20° to 40°C.

$$s = \frac{2.503 \times 10^6 \ \exp\left(\frac{17.27\,T_{air}}{T_{air}+237.3}\right)}{\left(T_{air} + 237.3\right)^2} \tag{64}$$

where:
s = slope of saturation vapor pressure temperature curve, Pa·K^{-1}
T_{air} = ambient temperature, °C

2.9.3 Latent heat of vaporization of water

The enthalpy of vaporization (i.e., the latent heat of vaporization) of water has a dependency on temperature given by (Henderson-Sellers 1984, Eq. 8):

$$L_v = 1.91846 \times 10^6 \ \left[\frac{T_{air} + 273.15}{(T_{air} + 273.15) - 33.91}\right]^2 \tag{65}$$

where:
L_v = latent heat of vaporization of water, J·kg^{-1}

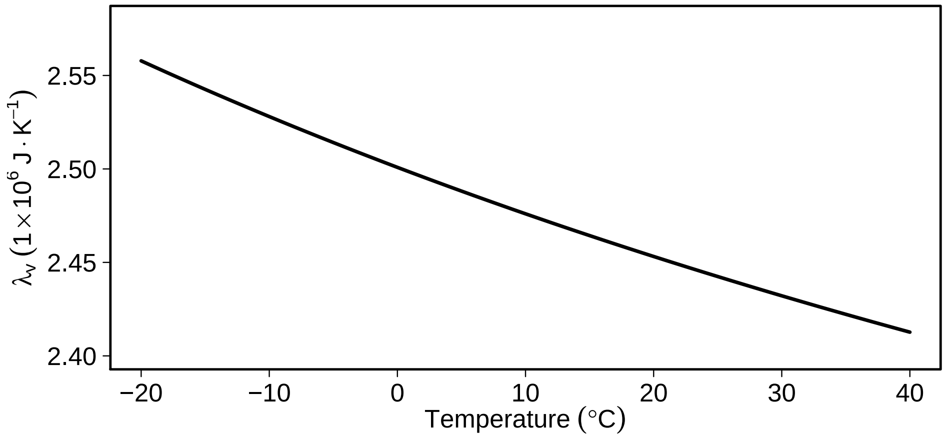

Figure 10: The latent heat of vaporization (1×10^6 J·kg^{-1}) at temperatures from -20° to 40°C.

T_{air} = ambient temperature, °C

2.9.4 Density of water

The density of water depends on the temperature and (weakly) on the pressure (Chen et al. 1977):

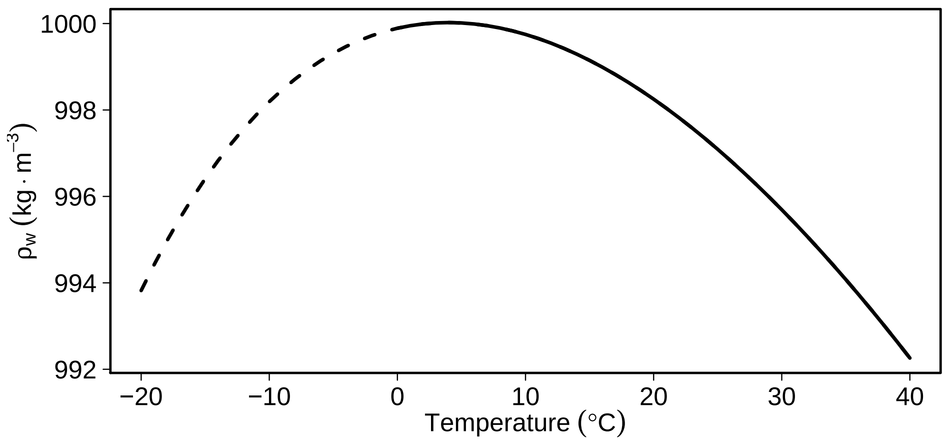

Figure 11: The density of water at sea-level for temperatures from −20° to 40°C (frozen water shown as dashed line).

$$\rho_w = 1000\,\rho_o\,\frac{K_o + C_A\,P^*_{atm} + C_B\,{P^*_{atm}}^2}{K_o + C_A\,P^*_{atm} + C_B\,{P^*_{atm}}^2 - P^*_{atm}} \tag{66}$$

where:
ρ_w = density of water, kg·m^{-3}
ρ_o = density of water at 1 atm, g·cm^{-3}
K_o = bulk modulus of water at 1 atm, bar
C_A = temperature-dependent coefficient, unitless
C_B = temperature-dependent coefficient, bar^{-1}
P^*_{atm} = atmospheric pressure, bar

The constant in Eq. 66 converts the units of density from g·cm^{-3} to kg·m^{-3}. The following relationship may be used to convert between the units of atmospheric pressure: 1 bar = 1 × 10^5 Pa. The density of water at 1 atm may be calculated as (Chen et al. 1977; Kell 1975):

$$\begin{aligned}\rho_o =& 0.99983952 + 6.78826\times10^{-5}\,T_{air}\\ &- 9.08659\times10^{-6}\,{T_{air}}^2 + 1.02213\times10^{-7}\,{T_{air}}^3\\ &- 1.35439\times10^{-9}\,{T_{air}}^4 + 1.47115\times10^{-11}\,{T_{air}}^5\\ &- 1.11663\times10^{-13}\,{T_{air}}^6 + 5.04407\times10^{-16}\,{T_{air}}^7\\ &- 1.00659\times10^{-18}\,{T_{air}}^8\end{aligned} \tag{67}$$

where:
ρ_o = density of water at 1 atm, g·cm^{-3}
T_{air} = ambient temperature, °C

The bulk modulus of water at 1 atm may be calculated as (Chen et al. 1977; Kell 1975):

$$\begin{aligned}K_o =& 19652.17 + 148.183\,T_{air} - 2.29995\,{T_{air}}^2 + 0.01281\,{T_{air}}^3\\ &- 4.91564\times10^{-5}\,{T_{air}}^4 + 1.03553\times10^{-7}\,{T_{air}}^5\end{aligned} \tag{68}$$

where:
K_o = bulk modulus of water at 1 atm, bar
T_{air} = ambient temperature, °C

The temperature-dependent coefficients, C_A and C_B, are defined as (Chen et al. 1977):

$$\begin{aligned}C_A =& 3.26138 + 5.223\times10^{-4}\,T_{air} + 1.324\times10^{-4}\,{T_{air}}^2\\ &- 7.655\times10^{-7}\,{T_{air}}^3 + 8.584\times10^{-10}\,{T_{air}}^4\end{aligned} \tag{69}$$

$$
\begin{aligned}
C_B =& 7.2061 \times 10^{-5} - 5.8948 \times 10^{-6}\, T_{air} + 8.699 \times 10^{-8}\, {T_{air}}^2 \\
& - 1.01 \times 10^{-9}\, {T_{air}}^3 + 4.322 \times 10^{-12}\, {T_{air}}^4
\end{aligned}
\tag{70}
$$

where:

C_A = temperature-dependent coefficient, unitless
C_B = temperature-dependent coefficient, bar^{-1}
T_{air} = ambient temperature, °C

2.9.5 Psychrometric constant

The psychrometric constant depends on both the temperature and pressure. The pressure dependency is defined as (Allen et al. 1998, Eq. 8):

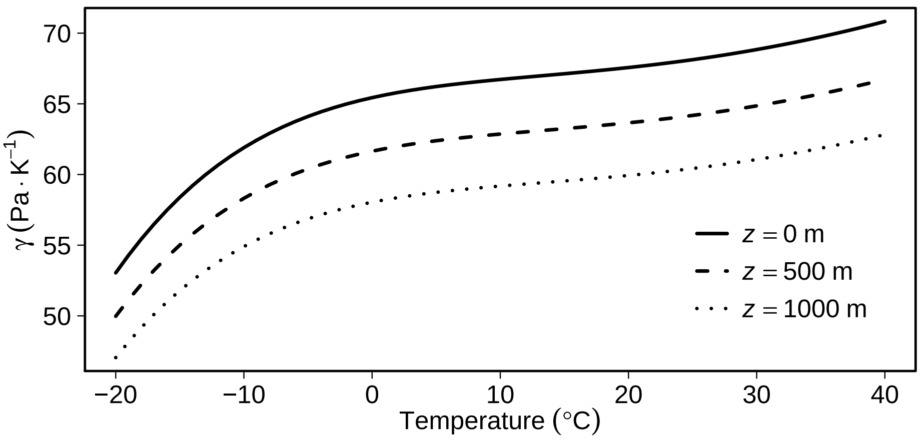

Figure 12: The psychrometric constant at three elevations for temperatures from −20° to 40°C.

$$\gamma = \frac{C_p\, M_a\, P_{atm}}{M_v\, L_v} \tag{71}$$

where:

γ = psychrometric constant, $\text{Pa}\cdot\text{K}^{-1}$
C_p = specific heat capacity of humid air, $\text{J}\cdot\text{kg}^{-1}\cdot\text{K}^{-1}$
M_a = molecular weight of dry air, $\text{kg}\cdot\text{mol}^{-1}$
M_v = molecular weight of water vapor, $\text{kg}\cdot\text{mol}^{-1}$
P_{atm} = atmospheric pressure, Pa
L_v = latent heat of vaporization of water, $\text{J}\cdot\text{kg}^{-1}$

Standard constants for M_a and M_v are given in Table 1. The latent heat of vaporization may either be assumed constant (e.g., $L_v \approx 2.5 \times 10^6$ J·kg^{-1}) or it can be calculated (see §2.9.3). The specific heat capacity of humid air may either be assumed constant (e.g., $C_p \approx 1.013 \times 10^3$ J·kg^{-1}·K^{-1}) or it can be calculated as a function of temperature (Tsilingiris 2008, Eq. 47):

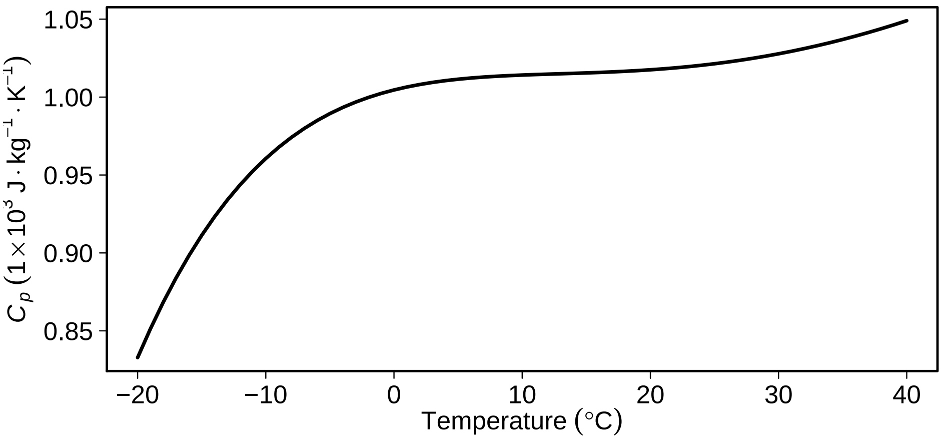

Figure 13: The specific heat capacity (1×10^3 J·kg^{-1}·K^{-1}) of humid air at temperatures from $-20°$ to 40°C.

$$\begin{aligned} C_p = 1000\,(1.0045714270 &+ 2.050632750 \times 10^{-3}\, T_{air} \\ &- 1.631537093 \times 10^{-4}\, {T_{air}}^2 + 6.212300300 \times 10^{-6}\, {T_{air}}^3 \\ &- 8.830478888 \times 10^{-8}\, {T_{air}}^4 + 5.071307038 \times 10^{-10}\, {T_{air}}^5) \end{aligned} \tag{72}$$

where:
C_p = specific heat capacity of humid air, J·kg^{-1}·K^{-1}
T_{air} = ambient temperature, °C

2.10 Condensation

Condensation may be assumed equal to the water-equivalent of the nighttime net radiant energy (see §2.7):

$$C_n = 1 \times 10^3\, E_{con}\, |H_N^*| \tag{73}$$

where:
C_n = daily nighttime condensation, mm
E_{con} = water to energy conversion factor, m^3·J^{-1}
H_N^* = daily nighttime total net radiation, J·m^{-2}

2.11 Equilibrium Evapotranspiration Rate

The equilibrium evapotranspiration (EET) rate may be calculated as the water-equivalent of the net daytime radiation (Prentice et al. 1993, Eq. 5):

$$E^q = 3.6 \times 10^6 \, E_{con} \, I_N \tag{74}$$

where:
E^q = equilibrium evapotranspiration rate, mm·h^{-1}
E_{con} = water to energy conversion factor, m^3·J^{-1}
I_N = net radiation flux, W·m^{-2}

Note that the constant in Eq. 74 converts the units from m·s^{-1} to mm·h^{-1}. There is no physical meaning for negative EET, and therefore EET should be set equal to zero when I_N is negative.

2.12 Daily Equilibrium Evapotranspiration

The daily total equilibrium evapotranspiration can be calculated, as in §2.11, as the water-equivalent of the daily daytime net radiation (i.e., §2.6):

$$E_n^q = 1 \times 10^3 \, E_{con} \, H_N \tag{75}$$

where:
E_n^q = daily equilibrium evapotranspiration, mm
E_{con} = water to energy conversion factor, m^3·J^{-1}
H_N = daily total net radiation, J·m^{-2}

Note that the constant in Eq. 75 converts the units from meters to millimeters.

2.13 Potential Evapotranspiration Rate

The potential evapotranspiration (PET) rate, E^p, may exceed the equilibrium evapotranspiration rate (i.e., Eq. 74) by an entrainment factor (Lhomme 1997; Priestley and Taylor 1972):

$$E^p = (1 + \omega) \; E^q \tag{76}$$

where:
E^p = potential evapotranspiration rate, mm·h^{-1}
E^q = equilibrium evapotranspiration rate, mm·h^{-1}
ω = entrainment factor, unitless

Setting the entrainment factor, ω, equal to zero sets E^p equal to E^q. A value of ω is given Table 1.

2.14 Daily Potential Evapotranspiration

The daily total potential evapotranspiration is calculated by scaling the daily total equilibrium evapotranspiration (i.e., §2.12) by the entrainment factor, ω:

$$E_n^p = (1 + \omega)\ E_n^q \tag{77}$$

where:
E_n^p = daily potential evapotranspiration, mm
E_n^q = daily equilibrium evapotranspiration, mm
ω = entrainment factor, unitless

2.15 Evaporative Demand

The instantaneous evaporative demand is based on the potential evapotranspiration (Federer 1982):

$$D_p = E^p = (1 + \omega)\ E^q \tag{78}$$

where:
D_p = evaporative demand rate, mm·h^{-1}
E^p = potential evapotranspiration rate, mm·h^{-1}
E^q = equilibrium evapotranspiration rate, mm·h^{-1}

The evaporative demand, D_p may also be expressed in terms of radiation fluxes. Based on Eq. 74, EET is related to the net radiation flux, which, based on Eq. 45, is the difference between net shortwave, I_{SW} and net longwave, I_{LW} radiation fluxes. The net shortwave radiation flux is related to the extraterrestrial radiation flux, I_o, through Eq. 47 and Eq. 46, such that D_p may be expressed as:

$$D_p = 3.6 \times 10^6\ (1 + \omega)\ E_{con}\ [(1 - \beta_{sw})\ \tau\ I_o - I_{LW}] \tag{79}$$

where:
ω = entrainment factor, unitless
β_{sw} = shortwave albedo, unitless
τ = atmospheric transmittivity, unitless
I_o = extraterrestrial solar radiation flux, W·m^{-2}
I_{LW} = net longwave radiation, W·m^{-2}
E_{con} = water to energy conversion factor, m^3·J^{-1}

Note the constants in Eq. 79 convert the units from m·s^{-1} to mm·h^{-1}. The total daily demand is based on E_n^p (i.e., §2.14) or the total daily daytime net radiation (i.e., §2.6):

$$D = (1+\omega)\ E_n^q = 1 \times 10^3\ (1+\omega)\ E_{con}\ H_N \tag{80}$$

where:

D = evaporative demand, mm

E_n^q = daily equilibrium evapotranspiration, mm

H_N = daily daytime net radiation, J·m^{-2}

2.16 Actual Evapotranspiration Rate

The actual evapotranspiration rate, E^a, is based on the minimum of the supply and demand rates, as shown in Fig. 14, (ibid., Eq. 7):

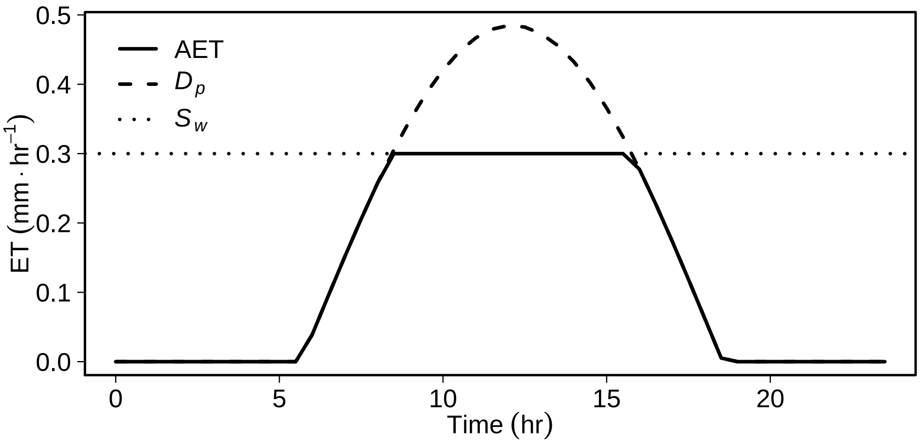

Figure 14: Example of the E^a for a given D_p when $S_w = 0.3$ mm·h^{-1}.

$$E^a = \min\left(S_w,\ D_p\right) \tag{81}$$

where:

E^a = actual evapotranspiration rate, mm·h^{-1}

S_w = evaporative supply rate, mm·h^{-1}

D_p = evaporative demand rate, mm·h^{-1}

Note that the minimization is based on the instantaneous rates and not the daily totals!

2.17 Daily Actual Evapotranspiration

The daily actual evapotranspiration can be analytically solved similar to the methods used for H_o (i.e., §2.4) and H_N (i.e., §2.6). Analogous to the sunset hour angle, h_s, and net radiation flux cross-over hour angle, h_n, a new hour angle must be defined relating to the point when $D_p = S_w$. This intersection hour angle, h_i, is found by setting the equation for D_p equal to S_w. Using the variable substitutions defined in §2.6 and letting $r_x = 3.6 \times 10^6\ (1+\omega)\ E_{con}$, D_p may be expressed as:

$$D_p = r_x\ \left[r_w\ (r_u + r_v\ \cos h) - I_{LW}\right] \tag{82}$$

Setting Eq. 82 equal to S_w and solving for the hour angle:

$$h_i = \arccos\left(\frac{S_w}{r_x\, r_w\, r_v} + \frac{I_{LW}}{r_w\, r_v} - \frac{r_u}{r_v}\right) \tag{83}$$

where:
h_i = supply and demand intersecting hour angle, radians
S_w = evaporative supply rate, mm·h^{-1}
$r_u = \sin\delta \cdot \sin\phi$, unitless
$r_v = \cos\delta \cdot \cos\phi$, unitless
$r_w = (1-\beta_{sw})\ \tau\ I_{sc}\, d_r$, W·m^{-2}
$r_x = 3.6 \times 10^6\ (1+\omega)\ E_{con}$, mm·m^2·W^{-1}·h^{-1}

Special care needs to be made when $\cos(h_i) \geq 1$ (i.e., supply rate exceeds demand, $h_i = 0$) and when $\cos(h_i) \leq -1$ (i.e., supply rate limits demand everywhere, $h_i = \pi$). Note that as S_w approaches zero, h_i approaches h_n (i.e., Eq. 55).

The half-day integral of actual evapotranspiration consists of two parts: the S_w curve from solar noon, h_o, to the intersection hour angle, h_i, and the D_p curve from h_i to the net radiation cross-over angle, h_n:

$$\int_{h_o}^{h_n} E^a = \int_{h_o}^{h_i} S_w + \int_{h_i}^{h_n} D_p \tag{84}$$

Integrating Eq. 84 and using the variable substitution as in Eq. 83:

$$\begin{aligned}\int_{h_o}^{h_n} E^a =& S_w\, h_i + r_x\, r_w\, r_v\ (\sin h_n - \sin h_i) \\ &+ r_x\ (r_w\, r_u - I_{LW})\ (h_n - h_i)\end{aligned} \tag{85}$$

Note that when S_w exceeds D_p (i.e., $h_i = 0$), Eq. 85 becomes equivalent to Eq. 80.

The daily actual evapotranspiration, E_n^a, is found by doubling the quantity in Eq. 85 and converting the units integrated over from radians to hours:

$$E_n^a = \frac{24}{\pi} \left[S_w \, h_i + r_x \, r_w \, r_v \, \left(\sin h_n - \sin h_i \right) \right. \\ \left. + \left(r_x \, r_w \, r_u - r_x \, I_{LW} \right) \left(h_n - h_i \right) \right] \tag{86}$$

where:
- E_n^a = daily actual evapotranspiration, mm
- S_w = evaporative supply rate, mm·hr^{-1}
- h_i = supply and demand intersecting hour angle, radians
- h_n = net radiation flux cross-over hour angle, radians
- $r_u = \sin\delta \cdot \sin\phi$, unitless
- $r_v = \cos\delta \cdot \cos\phi$, unitless
- $r_w = (1 - \beta_{sw}) \; \tau \; I_{sc} \, d_r$, W·m^{-2}
- $r_x = 3.6 \times 10^6 \; (1 + \omega) \; E_{con}$, mm·m^2·W^{-1}·h^{-1}

2.18 Daily Soil Moisture

The daily soil moisture, W_n, is calculated by adding the daily precipitation, P_n, and daily condensation, C_n (see §2.10), to yesterday's soil moisture and subtracting the daily actual evapotranspiration, E_n^a (see §2.17) (Cramer and Prentice 1988):

$$W_n = W_{n-1} + P_n + C_n - E_n^a \tag{87}$$

where:
- W_n = daily soil moisture, mm
- P_n = daily precipitation, mm
- C_n = daily nighttime condensation, mm
- E_n^a = daily actual evapotranspiration, mm

Note that daily soil moisture may exceed the soil moisture capacity, W_m. In such a case, the excess water is considered runoff and may be calculated as the maximum of zero or the difference between daily soil moisture and the moisture capacity:

$$RO = \max\left(0, \, W_n - W_m\right) \tag{88}$$

where:
- RO = daily runoff, mm
- W_n = daily soil moisture, mm
- W_m = soil moisture capacity, mm

Following the runoff calculation, daily soil moisture must be set within the physical limits (i.e., $0 \leq W_n \leq W_m$) before calculating tomorrow's evaporative supply and soil moisture quantities:

$$W_n = \begin{cases} W_m, & \text{if } W_n \geq W_m \\ 0, & \text{if } W_n \leq 0 \end{cases} \tag{89}$$

2.19 Cramer-Prentice Moisture Index

The Cramer-Prentice bioclimatic moisture index, α, is calculated as (as described in Gallego-Sala et al. 2010; Sykes et al. 1996):

$$\alpha = \frac{E_m^a}{E_m^q} \tag{90}$$

where:
α = monthly Cramer-Prentice moisture index, unitless
E_m^a = monthly actual evapotranspiration, mm
E_m^q = monthly potential evapotranspiration, mm

Note E_m^a and E_m^q are the cumulative E_n^a and E_n^q for a given month.

Due to the fact that E^a follows E^p during the course of the day and given the definition of E_n^p (see §2.14), the value of α is expected to range between 0 and $1 + \omega$ (e.g., 1.26, when $\omega = 0.26$).

2.20 Climatic Water Deficit

The climatic water deficit is a measure of the difference between actual and potential evapotranspiration (Stephenson 1998):

$$\Delta E_m = E_m^p - E_m^a \tag{91}$$

where:
ΔE_m = monthly climatic water deficit, mm
E_m^a = monthly actual evapotranspiration, mm
E_m^p = monthly potential evapotranspiration, mm

A Python Code

A.1 Julian Day

```
01  def julian_day(y, m, i):
02    if m <= 2:
03       y = y-1
04       m = m+12
05    A = int(y/100)
06    B = 2-A+int(A/4)
07    JDE = int(365.25*(y+4716))+int(30.6001*(m+1))+i+B-1524.5
08    return(JDE)
```

This script calculates the Julian day for a given date in the Gregorian calendar (Meeus 1991, Ch. 7), where `y` is the year, `m` is the month (i.e., 1–12), and `i` is the day (i.e., 1–31). The term B on Line 06 is for the modified definition of leap-years in the Gregorian calendar from the Julian calendar. If using the Julian calendar dates, set B equal to zero. To test whether the algorithm is correctly implemented, the Julian day of 13 Aug 2014 is 2456882.

A.2 Equinox

```
def equinox(y, opt=0):
  # Table 26.A: jde_table_a
  # Table 26.B: jde_table_b
  # Table 26.C: periodic_terms
  if y < 1000:
     jde_table = jde_table_a
     y = y/1000.0
  else:
     jde_table = jde_table_b
     y = (y-2000.0)/1000.0
  jde0 = (
     jde_table[opt,0] +
     jde_table[opt,1]*y +
     jde_table[opt,2]*y**2 +
     jde_table[opt,3]*y**3 +
     jde_table[opt,4]*y**4
  )
  t = (jde0-2451545.0)/36525.0
  w = (35999.373*t)-2.47
  dl = (
     1.0 +
     (0.0334 * numpy.cos(numpy.pi/180*w)) +
     (0.0007 * numpy.cos(numpy.pi/180*2*w))
  )
  s = 0
  j = 0
  for i in xrange(24):
     s += periodic_terms[j]*numpy.cos(
        numpy.pi/180.0*(
           periodic_terms[j+1] +
           (periodic_terms[j+2]*t)
        )
     )
     j=j+3
  jde = jde0+((s*0.00001)/dl)
  jde_year = julian_day(y, 1, 1)
  return (jde-jde_year+1)
```

This algorithm calculates the corresponding Julian day of the vernal equinox (i.e., `opt=0`) for a given year (Meeus 1991, Ch. 26). In this example, numpy is used for defining the arrays, calculating the cosine, and for the numerical definition of π. The three tables that are referenced on Lines 02–04 need to be defined.

References

Abbot, C. G. (1914). “The solar constant of radiation”. In: *Science* 39.1001, pp. 335–348 (cit. on p. 14).

Abbot, C. G. and F. E. Fowle Jr. (1911). “The value of the solar constant of radiation”. In: *The Astrophysical Journal* 33.3, pp. 191–196 (cit. on p. 14).

Allen, C. W. (1973). *Astrophysical Quantities*. 3rd ed. London: The Athlone Press (cit. on pp. 10, 15).

Allen, R. G. (1996). “Assessing integrity of weather data for reference evapotranspiration estimation”. In: *Journal of Irrigation and Drainage Engineering* 122, pp. 97–106 (cit. on p. 28).

Allen, R. G., L. S. Pereira, D. Raes, and M. Smith (1998). *Crop evapotranspiration - Guidelines for computing crop water requirements - FAO irrigation and drainage paper 56*. Tech. rep. Rome: Food and Agriculture Organization of the United Nations. URL: `http://www.fao.org/docrep/x0490e/x0490e00.htm` (cit. on pp. 33, 34, 37).

Berger, A. L. (1977). “Support for the astronomical theory of climate change”. In: *Nature* 269, pp. 44–45 (cit. on p. 17).

Berger, A. L. (1978). “Long-term variations of daily insolation and quaternary climatic changes”. In: *Journal of the Atmospheric Sciences* 35, pp. 2362–2367 (cit. on pp. 10, 22).

Cavcar, M. (2000). *The International Standard Atmosphere (ISA)*. Tech. rep. Eskisehir, Turkey: Anadolu University. URL: `http://home.anadolu.edu.tr/~mcavcar/common/ISAweb.pdf` (cit. on p. 10).

Chen, C.-T., R. A. Fine, and F. J. Millero (1977). “The equation of state of pure water determined from sound speeds”. In: *The Journal of Chemical Physics* 66, pp. 2142–2144 (cit. on pp. 35, 36).

Cooper, P. I. (1969). “The absorption of radiation in solar stills”. In: *Solar Energy* 12.3, pp. 333–346 (cit. on pp. 18, 19).

Cramer, W. and I. C. Prentice (1988). “Simulation of regional soil moisture deficits on a European scale”. In: *Norsk Geografisk Tidsskrift - Norwegian Journal of Geography* 42.2–3, pp. 149–151 (cit. on pp. 8, 11, 43).

Crommelynck, D. and S. Dewitte (1997). “Solar constant temporal and frequency characteristics”. In: *Solar Physics* 173, pp. 177–191 (cit. on p. 14).

Dewitte, S., D. Crommelynck, S. Mekaoui, and A. Joukoff (2004). “Measurement and uncertainty of the long-term total solar irradiance trend”. In: *Solar Physics* 224, pp. 209–216 (cit. on p. 14).

Duffie, J. A. and W. A. Beckman (2013). *Solar engineering of thermal processes*. 4th ed. New Jersey: John Wiley and Sons (cit. on pp. 13, 16, 17).

Federer, C. A. (1968). “Spatial variation of net radiation, albedo and surface temperature of forests”. In: *Journal of Applied Meteorology* 7, pp. 789–795 (cit. on p. 10).

Federer, C. A. (1982). "Transpirational supply and demand: plant, soil, and atmospheric effects evaluated by simulation". In: *Water Resources Research* 18.2, pp. 355–362 (cit. on pp. 10, 13, 40, 41).

Fröhlich, C. (2006). "Solar irradiance variability since 1978: Revision of the PMOD composite during solar cycle 21". In: *Space Science Research* 125, pp. 53–65 (cit. on p. 14).

Gallego-Sala, A. V., J. M. Clark, J. I. House, H. G. Orr, I. C. Prentice, P. Smith, T. Farewell, and S. J. Chapman (2010). "Bioclimatic envelope model of climate change impacts on blanket peatland distribution in Great Britain". In: *Climate Research* 45, pp. 151–162 (cit. on p. 44).

Harris, I., P. D. Jones, T. J. Osborn, and D. H. Lister (2014). "Updated high-resolution grids of monthly climatic observations - the CRU TS3.10 Dataset". In: *International Journal of Climatology* 34.3, pp. 623–642 (cit. on p. 9).

Hays, J. D., J. Imbrie, and N. J. Shackleton (1976). "Variations in the earth's orbit: Pacemaker of the Ice Age". In: *Science* 194, pp. 1121–1132 (cit. on p. 17).

Henderson-Sellers, B. (1984). "A new formula for latent heat of vaporization of water as a function of temperature". In: *Quarterly Journal of the Royal Meteorological Society* 110, pp. 1186–1190 (cit. on p. 34).

Iqbal, M. (1983). "1. An Introduction to Solar Radiation". In: New York: Academic Press, Inc. Chap. Sun—Earth Astronomical Relationship (cit. on p. 20).

Kell, G. S. (1975). "Density, thermal expansivity, and compressibility of liquid water from 0° to 150°C: Correlations and tables for atmospheric pressure and saturation reviewed and expressed on 1968 temperature scale". In: *Journal of Chemical and Engineering Data* 20.1, pp. 97–105 (cit. on p. 36).

Klein, S. A. (1977). "Calculation of monthly average insolation on tilted surfaces". In: *Solar Energy* 19, pp. 325–329 (cit. on p. 16).

Kopp, G. and J. L. Lean (2011). "A new, lower value of total solar irradiance: Evidence and climate significance". In: *Geophysical Research Letters* 38.L01706 (cit. on pp. 10, 14).

Krivova, N. A., L. E. A. Vieira, and S. K. Solanki (2010). "Reconstruction of solar spectral irradiance since the Maunder minimum". In: *Journal of Geophysical Research* 115.A12112 (cit. on p. 14).

Kutzbach, J. E. and R. G. Gallimore (1988). "Sensitivity of a coupled atmosphere/mixed layer ocean model to changes in orbital forcing at 9000 years B.C." In: *Journal of Geophysical Research* 93.D1, pp. 803–821 (cit. on p. 23).

Lhomme, J.-P. (1997). "A theoretical basis for the Priestley-Taylor coefficient". In: *Boundary Layer Meteorology* 82, pp. 179–191 (cit. on pp. 10, 39).

Linacre, E. T. (1968). "Estimating the net-radiation flux". In: *Agricultural Meteorology* 5, pp. 49–63 (cit. on pp. 10, 27–29).

Loutre, M. F. (2002). "Encyclopedia of Atmospheric Sciences". In: Elsevier Science, Ltd. Chap. Ice age (Milankovitch Theory (cit. on pp. 15, 17).

Meek, D. W., J. L. Hatfield, T. A. Howell, S. B. Idso, and R. J. Reginato (1984). "A generalized relationship between photosynthetically active radiation and solar radiation". In: *Agronomy Journal* 76, pp. 939–945 (cit. on p. 10).

Meeus, J. (1991). *Astronomical algorithms*. 1st ed. Virginia: Willmann-Bell, Inc. (cit. on pp. 12, 13, 45, 46).

Monteith, J. L. and M. H. Unsworth (1990). *Principles of Environmental Physics*. 2nd ed. Oxford: Butterworth-Heinemann (cit. on p. 10).

Oglesby, M. (Feb. 1998). *Fourier paper*. Online. URL: `https://www.mail-archive.com/sundial@uni-koeln.de/msg01050.html` (cit. on p. 20).

Prentice, I. C., M. T. Sykes, and W. Cramer (1993). "A simulation model for the transient effects of climate change on forest landscapes". In: *Ecological Modelling* 65, pp. 51–70 (cit. on p. 39).

Priestley, C. H. B. and R. J. Taylor (1972). "On the assessment of surface heat flux and evaporation using large-scale parameters". In: *Monthly Weather Review* 100.2, pp. 81–92 (cit. on pp. 10, 39).

Sellers, P. J. (1985). "Canopy reflectance, photosynthesis and transpiration". In: *International Journal of Remote Sensing* 6.8, pp. 1335–1372 (cit. on p. 10).

Spencer, J. W. (1971). "Fourier series representation of the position of the sun". In: *Search* 2, p. 172. URL: `http://www.mail-archive.com/sundial@uni-koeln.de/msg01050.html` (cit. on pp. 19, 20).

Stephenson, N. L. (1998). "Actual evapotranspiration and deficit: biologically meaningful correlates of vegetation distribution across spatial scales". In: *Journal of Biogeography* 25, pp. 855–870 (cit. on p. 44).

Stine, W. B. and M. Geyer (2001). "Power from the Sun". In: Available online: `http://www.powerfromthesun.net/Book/chapter03/chapter03.html`. Author. Chap. 3. The sun's position (cit. on pp. 19–21).

Sykes, M. T., I. C. Prentice, and W. Cramer (1996). "A bioclimatic model for the potential distributions of north European tree species under present and future climates". In: *Journal of Biogeography* 23, pp. 203–233 (cit. on p. 44).

Tsilingiris, P. T. (2008). "Thermophysical and transport properties of humid air at temperature range between 0 and 100 °C". In: *Energy Conversion and Management* 49, pp. 1098–1110 (cit. on pp. 10, 38).

Wetherald, R. T. and S. Manabe (1972). "Response of the joint ocean-atmosphere model to the seasonal variation of the solar radiation". In: *Monthly Weather Review* 100.1, pp. 42–59 (cit. on p. 17).

Willson, R. C. (1997). "Total solar irradiance trend during solar cycles 21 and 22". In: *Science* 277, pp. 1963–1965 (cit. on p. 14).

Woolf, H. M. (1968). *On the computation of solar evaluation angles and the determination of sunrise and sunset times*. Tech. rep. NASA-TM-X-164. National Aeronautics and Space Administration (NASA). URL: `http://ntrs.nasa.gov/search.jsp?R=19680025707` (cit. on pp. 17, 20, 21).